2
Stokesian locomotion

We turn to the locomotion of bodies as small Reynolds numbers, the fluid dynamics being that of the Stokes equations (**??**). Assuming constant density and viscosity, these equations are

$$\nabla p - \mu \nabla^2 \mathbf{u} = 0, \quad \nabla \cdot \mathbf{u} = 0. \tag{2.1}$$

Having dropped completely the inertia of the fluid, including the linear time derivative, we pass to a world where dynamical equilibration is instantaneous. In the familiar Newtonian world, an imposed force accelerates a body, and the change of velocity requires a finite time. As inertia tends to zero, the response becomes instantaneous and the viscous and pressure forces must be in dynamic equilibrium at every instant.

Formally, the Stokesian realm is the limit of Navier-Stokes theory for small Reynolds number $Re = UL/\nu$, it being understood that time scales of the flow are of order L/U. In the natural setting small Reynolds number occurs because of small *size*, typically microorganisms and tiny insects. Since body densities in these settings are not to far different from the fluid density, body inertia is also negligible. Thus the system of fluid and body comprising the domain of locomotion is one of negligible inertia, and we shall always include the body within the Stokesian approximation.

The most dramatic result of this equilibrium is that, for free swimming in the Stokesian realm, and without any external force such as gravity, the force exerted by the fluid on the body is identically zero at each instant of time. For, a non-zero force cannot be balanced by any inertial response of the body. Conversely, the force exerted on the fluid by a free Stokesian swimmer is identically zero. The Stokesian realm emphasizes the fundamen-

tal distinction between the forces on body and fluid, and the locomotion of the body relative to the fluid.

Although formally the time variable has disappeared from the equations of motion, time does linger here as a *parameter*. That is, time is needed as a label for the state of the Stokesian system as determined by the instantaneous geometry and boundary conditions. In locomotion, our concern is usually the exterior of a three-dimensional deformable body. As the body deforms, we may speak of sequence of body configurations and Stokes flows determined by the instantaneous body motion. Thus the time now serves as a parameter attached to this sequence of configurations.

In the present chapter we shall examine some properties of the Stokes equations and then develop several theories for locomotion in the Stokesian realm.

2.1   The exterior problem for the Stokes equations

To study a locomoting body in the Stokesian realm we need to solve the Stokes equations with the velocity given on the instantaneous body surface S.

$$\mathbf{u}|_S = \mathbf{u}_S(\mathbf{x}), \tag{2.2}$$

together with the condition that the velocity vanish at infinity,

$$\mathbf{u}_\infty = 0. \tag{2.3}$$

It is known that for sufficiently smooth S and $\mathbf{u}_s$ there exists a unique solution to this problem, see e.g. [8]. This solution can be given explicitly only in a few simple cases, for example for the classical problem of Stokes of uniform flow past a sphere. Other examples are given in [7].

The uniqueness of the solution is important for understanding the mechanics of Stokesian locomotion. Essential here is the linearity of the Stokes equation. The difference $\mathbf{v}$ of two solutions then satisfies the Stokes equations with $\mathbf{v}_S = 0$. The dot product $\mathbf{v} \cdot (\nabla p - \mu \, lap\mathbf{v})$, when integrated over the region between the body and a large sphere of radius R, yields a vanishing contribution on S, and a vanishing contribution on the distant sphere provided that $\mathbf{v}$ and p decay sufficiently fast. It is sufficient in three dimensions that $\mathbf{v} = O(r^{-1}, \nabla \mathbf{v} = O(r^{-2})$, and $p = O(r^{-2})$, which are obtained by solutions. We are thus left with an integral of $\left(\frac{\partial v_i}{\partial x_j}\right)^2$ over the exterior regions equal to zero. This implies $\mathbf{v} = \text{constant} = 0$.

To see something of the structure of exterior solutions of the Stokes equations, we consider first a simple potential field $\mathbf{u} = \nabla \phi$, which is solenoidal provided that $\nabla^2 \phi = 0$, i.e ϕ is a harmonic function of $\mathbf{x}$. This field is clearly the velocity field of a Stokes flow with a constant pressure. Note that although the viscous force vanishes identically in such a Stokes flow, viscous stresses are non-zero.

A richer class of solutions have a velocity field in the component form

$$u_i = [\frac{\partial^2 \chi}{\partial x_i \partial x_j} - \nabla^2 \chi \delta_{ij}]a_j \tag{2.4}$$

where $\mathbf{a}$ is a constant vector. The corresponding pressure will be

$$p = \mu \frac{\partial \nabla^2 \chi}{\partial x_j} a_j. \tag{2.5}$$

Note that the form of $\mathbf{u}$ insures that it is divergence-free, and that the pressure is in equilibrium with the viscous force associated with the first term on the right of (2.4). The Stokes equations are thus satisfied by (2.4) and (2.5) provided that

$$\nabla^4 \chi = 0, \tag{2.6}$$

i.e. if χ is a *biharmonic function*. A large class of solutions relevant to the exterior problem can thus be found by separation of variables, for example, in spherical polar coordinates. As an example, we give the classical solution of Stokes for flow of a fluid with velocity $(U, 0, 0)$ past a solid sphere of radius r_0 on which the non-slip condition is satisfied. The velocity field is a linear combination of (2.4) with $\chi = r$ and a potential field with dipole potential:

$$\mathbf{u} = U\mathbf{i} + A(x\mathbf{r}r^{-3} + r^{-1}\mathbf{i}) + B\nabla(xr^{-3}). \tag{2.7}$$

We see that $\mathbf{u} = 0$ on $r = r_0$ provided that $A = -\frac{3}{4}r_0 U, B = -\frac{1}{4}r_0^3 U$. Note that as a generalized function $\nabla^4 r = -8\pi\delta(\mathbf{x})$. Thus the field (2.4) within $\chi = r$ is the velocity caused by a point force of strength $-8\pi\mu\mathbf{a}$ acting at the origin. From the value of A and the fact that the harmonic dipole will not contribute to the point force we conclude that the drag acting upon the sphere is $8\pi\mu \times \frac{3}{4}r_0 U = 6\pi r_0 U\mu$, which is the famous result of Stokes.

As a third and final class of solutions, we consider

$$\mathbf{u} = \nabla\psi \times \mathbf{b}, \tag{2.8}$$

where $\mathbf{b}$ is a constant vector. This is a Stokes solution with constant a pressure provided that ψ is harmonic. As an example, when $\psi = r_0^3 r^{-1}$ (2.8) gives the flow due to a sphere of radius r_0 spinning with angular velocity $\mathbf{b}$.

Given the above special solutions, the question naturally arises as what family of solutions is sufficient to represent by superposition *any* solution of the exterior boundary-value problem. We discuss this issue now, by supposing that the unique solution is known from the body surface out to some sphere S_0 which contains the body. We are assured that if we can construct a solution of the Stokes equations exterior to S_0, such that the necessary values are assumed by the solution on S_0, then this constructed solution must agree with the original solution extended in the exterior of S_0. Thus

it is sufficient to solve the exterior problem for a sphere to ensure that we have a complete set of Stokes solutions.

Suppose now that $\mathbf{u}$ is divergence-free in the exterior V_0 of S_0, and let $r = (x^2 + y^2 + z^2)^{1/2}$ be the distance to the origin from a point in V_0, $r = r_0$ being S_0. We first show that two such fields with the same values of $\mathbf{r} \cdot \mathbf{u}$ and $\mathbf{r} \cdot (\nabla \times \mathbf{u})$ on every spherical surface $r = r_1 \geq r_0$, must agree throughout V_0. [1] Indeed, if $\mathbf{u}$ is divergence-free and $\mathbf{r} \cdot \mathbf{u} = r u_r = 0$, (u_r, u_θ, u_ϕ) being the velocity in spherical polar coordinates r, θ, ϕ, then the formula for divergence gives

$$\frac{\partial \sin \theta u_\theta}{\partial \theta} + \frac{\partial u_\phi}{\partial \phi} = 0. \tag{2.9}$$

If also $\mathbf{r} \cdot (\nabla \times \mathbf{u}) = 0$ in V_0, then

$$\frac{\partial \sin \theta u_\phi}{\partial \theta} - \frac{\partial u_\theta}{\partial \phi} = 0. \tag{2.10}$$

Combining the last two equations, we see that

$$L^2[u_\theta, u_\phi] = 0, \quad L^2 u = \frac{\partial}{\partial \theta}\left[\sin \theta\left(\frac{\partial (\sin \theta u)}{\partial \theta}\right)\right] + \frac{\partial^2 u}{\partial \phi^2}. \tag{2.11}$$

Multiplying $-L^2 u_\phi = 0$ by u_ϕ and integrating over a sphere $r = r_1 \geq r_0$ we obtain a positive definite quadratic implying $u_\phi = 0$ everywhere in V_0, and similarly for u_θ. Thus $\mathbf{u} = 0$ throughout V_0.

We now represent $\mathbf{u}$ in the form

$$\mathbf{u} = \nabla \times (\nabla \times \mathbf{r}P) + \nabla \times \mathbf{r}T, \tag{2.12}$$

involving the scalar functions P, T, and note that

$$\mathbf{r} \cdot \mathbf{u} = -\Lambda^2 P, \mathbf{r} \cdot (\nabla \times \mathbf{u}) = -\Lambda^2 T, \tag{2.13}$$

where

$$\Lambda^2 = \frac{\partial^2}{\partial \theta^2} + \cot \theta \frac{\partial}{\partial \theta} + \frac{1}{\sin^2 \theta} \frac{\partial^2}{\partial \phi^2}. \tag{2.14}$$

Thus if P, T can be found so that (2.13) are satisfied for the given $\mathbf{u}$, we know that any divergence-free velocity field can be represented in the form a(2.12).

To show that this is the case, we must consider the invertibility of the operator Λ^2. A suitable space of functions is the Hilbert space of complex scalar fields defined on the rectangle $R : \quad 0 \leq \theta \leq \pi, 0 \leq \phi \leq 2\pi$

---

[1] Here and throughout our work the necessary smoothness is assumed for all differentiations used. Any special considerations of regularity which are essential to the discussion will be dealt with explicitly as they arise.

and periodic with period 2π in ϕ, with inner product given by $(f, g) = \int_R f^* g \sin\theta d\theta d\phi$. Now Λ^2 is easily seen to be self-adjoint on this space, and to have eigenvalue 0 corresponding to a constant eigenfunction. Extended to all of V_0, this amounts to an eigenfunction which is an arbitrary function of $r \geq r_0$. It then follows that P, T are uniquely determined by (2.13) in V_0 provided that

$$\int_R [\mathbf{r} \cdot \mathbf{u}, \mathbf{r} \cdot (\nabla \times \mathbf{u})] \sin\theta d\theta d\phi = [0, 0]. \tag{2.15}$$

This is always the case provided fluid mass is not being added within S_0, e.g. if the body has fixed volume or if volume changes by adsorption of fluid. [2]

We thus have shown that $\mathbf{u}$ generally has the decomposition (2.12), and in particular this is true for Stokes flows solving our exterior problem. Since then

$$\nabla^2 \mathbf{u} = \nabla\nabla^2 (r\frac{\partial P}{\partial r} - P) - \mathbf{r}\nabla^4 P + \nabla(\nabla^2 T) \times \mathbf{r}, \tag{2.16}$$

we see that Stokes flows with velocity (2.12) require a pressure given by

$$p = \mu\nabla^2 (r\frac{\partial P}{\partial r} - P) \tag{2.17}$$

and that P and T satisfy

$$\nabla^4 P = 0, \nabla^2 T = 0. \tag{2.18}$$

We remark that it can be shown that any decomposition (2.12) can be built up from solutions of the form (2.4) and (2.8), see problem 2.1 below.

2.1.1   Solutions with symmetry

In special cases indicated by symmetry or a particular coordinate system, the derivation solutions of the Stokes equations can be derived from a single scalar streamfunction. We illustrate this by deriving the uniform Stokes flow past a sphere using spherical polar coordinates for $\mathbf{u} = (u_r, u_\theta, u_\phi)$ with $u_\phi = 0$ and the flow invariant in ϕ. In this case the Stokes equations take the form

$$\frac{\partial p}{\partial r} - \mu\left(\nabla^2 u_r - \frac{2u_r}{r^2} - \frac{2}{r^2 \sin\theta}\frac{\partial(u_\theta \sin\theta)}{\partial\theta}\right) = 0, \tag{2.19}$$

$$\frac{1}{r}\frac{\partial p}{\partial\theta} - \mu\left(\nabla^2 u_\theta + \frac{2}{r^2}\frac{\partial u_r}{\partial\theta} - \frac{u_\theta}{r^2 \sin^2\theta}\right) = 0, \tag{2.20}$$

---

[2]We remark that the decomposition (2.12) is usually referred to as a *poloidal (P), toroidal (T) decomposition* of a divergence-free field. It is particularly useful in spherical domains, and has been widely applied in the modeling of magnetic and velocity field of spherical bodies such as planets and stars, see e.g. [13], [1].

$$\frac{1}{r^2}\frac{\partial(r^2 u_r)}{\partial r} + \frac{1}{r\sin\theta}\frac{\partial(\sin\theta u_\theta)}{\partial\theta} = 0, \tag{2.21}$$

$$\nabla^2 Q = \frac{1}{r^2}\frac{\partial}{\partial r}\left(r^2\frac{\partial Q}{\partial r}\right) + \frac{1}{r^2\sin\theta}\frac{\partial}{\partial\theta}\left(\sin\theta\frac{\partial Q}{\partial\theta}\right) = 0. \tag{2.22}$$

We may satisfy the solenoidal condition (2.21) using the *Stokes stream-function* Ψ , defined by

$$u_r = \frac{1}{r^2\sin\theta}\frac{\partial\Psi}{\partial\theta}, \ u_\theta = -\frac{1}{r\sin\theta}\frac{\partial\Psi}{\partial r}. \tag{2.23}$$

Eliminating pressure from (2.19) and (2.20) and using (2.23) we obtain a fourth-order equation for Ψ. However the easiest way to get the result is to take the curl of the primitive Stokes equations, recognizing that for the symmetry of the flow leaves on the ϕ component of vorticity. The we have

$$\nabla^2\omega_\phi - \frac{\omega_\phi}{r^2\sin^2\theta} = 0, \ \omega_\phi = \frac{1}{r}\frac{\partial(r u_\theta)}{\partial r} - \frac{1}{r}\frac{\partial u_r}{\partial\theta}. \tag{2.24}$$

Now using (2.23) we get

$$\omega_\phi = -\frac{1}{r\sin\theta}L^2\Psi, \ L^2 Q \equiv \left[\frac{\partial^2}{\partial r^2} + \frac{\sin\theta}{r^2}\frac{\partial}{\partial\theta}\left(\frac{1}{\sin\theta}\frac{\partial}{\partial\theta}\right)\right]Q. \tag{2.25}$$

Using this result in (2.24) and employing (2.22) we arrive at

$$L^2(L^2\Psi) = 0. \tag{2.26}$$

For steady Stokes flow past a sphere of radius a we have the boundary conditions

$$\Psi_\theta(a,\theta) = 0, \ \Psi_r(a,\theta) = 0, \ \Psi \to \frac{1}{2}\sin^2\theta r^2, r\to\infty, \tag{2.27}$$

where $U\mathbf{i}$ is the velocity of the free stream.

We thus set $\Psi = f(r)\sin^2\theta$ to obtain

$$\left(\frac{d^2}{dr^2} - \frac{2}{r^2}\right)\left(\frac{d^2}{dr^2} - \frac{2}{r^2}\right)f = 0. \tag{2.28}$$

From the trial solution $f = r^n$ we see that $f = A/r + Br + Cr^2 + Dr^4$. From our conditions (2.27) we see that $D = 0$ and $C = \frac{1}{2}U$, and then that $B = \frac{3}{4}r_0 U, A = \frac{1}{4}r_0^3 U$. This gives us the Stokes streamfunction

$$\Psi = \left(\frac{1}{2}Ur^2 + \frac{1}{4}Ur_0^3 r^{-1} - \frac{3}{4}r_0 Ur\right)\sin^2\theta. \tag{2.29}$$

2.2 Calculation of force, torque, and rate of working

From the solution of the exterior problem we may compute the force and torque acting on the boundary S, and the instantaneous rate of viscous dissipation, equal to the instantaneous rate of working of S on the surrounding fluid (see problem 2.2). Now the local conservation of momentum and of angular momentum may be expressed in terms of the stress tensor σ as

$$\frac{\partial \sigma_{ij}}{\partial x_j} = 0, \quad \frac{\partial(\epsilon_{ijk}x_j\sigma_{kl})}{\partial x_l} = 0, \tag{2.30}$$

where $\sigma_{ij} = -p\delta_{ij} + \nu\left(\frac{\partial u_i}{\partial x_j} + \frac{\partial u_j}{\partial x_i}\right)$. The force and torque exerted by the fluid on the body are

$$F_i = \int_S \sigma_{ij}n_j dS, \; T_i = \int_S \epsilon_{ijk}x_j\sigma_{kl}n_l dS, \tag{2.31}$$

where $\mathbf{n}$ is the outward normal to the body.

The rate of working of the surface on the fluid is equal to the dot product of surface velocity $\mathbf{u}_S$ and force on fluid, integrated over the body surface,

$$W = -\int_S u_{Si}\sigma_{ij}n_j dS. \tag{2.32}$$

As an example, consider the rate of working per unit area of sheet for the stretching swimming sheet. From (??) and (??) we see that, to leading order,

$$W \approx -\langle \mu \frac{\partial u_1}{\partial y}(x,0,t)a\omega \sin(kx - \omega t)\rangle = \mu k a^2 \omega^2. \tag{2.33}$$

2.3 Locomotion

The essential feature of Stokesian locomotion that allows a rather complete analysis is the linearity of the fluid equations. This allows us write the complete flow as a sum of contributions each of which accommodates a portion of the physics. Suppose we are dealing with a deformable finite body in three dimensions with a prescribed standard shape. We can consider the flow set up in the standard frame, and the resulting force $\mathbf{F}_1(t)$ and torque $\mathbf{T}_1(t)$ exerted on the fluid by the body. These quantities may be computed at each instant from the uniquely defined Stokes flows existing at that instant.

Next we consider the force and torque generated by a rigid body motion. If the instantaneous translational velocity and angular velocity of the standard frame are $\mathbf{U}(t)$ and $\Omega(t)$ respectively, then by the linearity there

are non-singular matrices $\mathbf{A}(t), \mathbf{B}(t)$, determined by the standard shape at time t, such that $\mathbf{F}_2(t) = \mathbf{A} \cdot \mathbf{U}(t)$ is the force exerted on the fluid by virtue of its translation, and $\mathbf{T}_2)t) = \mathbf{B} \cdot \Omega(t)$ is the torque exerted on the fluid due to body spin. [3]

If the body is composed of a density comparable to that of the fluid, then the Stokes approximation applies to both fluid and body, so that inertial effects are negligible in both. In that case $\mathbf{F}_1(t) + \mathbf{F}_2(t) = 0$ and $\mathbf{T}_1(t) + \mathbf{T}_2(t) = 0$. These expressions may be regarded as equations for the instantaneous values of $\mathbf{U}$ and Ω, provided that the Stokes flows are all known. Thus the locomotion of the body can in principle be determined from the evolution of the standard shape.

If gravity is present, a third component of the motion comes from gravitational force and torque. In Stokes flow, the buoyancy force $g(M_{body} - \rho V_{body}$ will be balanced by a viscous drift force of order $\mu L U_{drift}$. The drift velocity will be negligible compared to the characteristic locomotion speed U provided that $(r_M - 1)Re/Fr^2 \ll 1$. For microorganisms the density contrast $r_M - 1$ is usually only a few percent, which tends to make gravity effect negligible in bacteria and spermatozoa, but non-negligible in the ciliated protozoa. The phenomenon of *bioconvection* is a gravity-mediated aspect of locomotion in some ciliates, see section ??.

2.4 Time-reversal symmetry, and the scallop theorem

Relative to the standard frame, the standard shape of a Stokesian locomoter can be thought of a path in certain space of configurations. That is, the instantaneous standard shape represented as a point in a *configuration space*, and the movements of the body as a line through this space. A periodic movement is a closed loop in the space.

Since time is a parameter in Stokes flow, the time at which a given configuration is assumed is a convenient parameter for the configuration path. At each time, there is a surface velocity associated with the instantaneous body movement in the standard frame, and there is an instantaneous, unique rigid body motion with make the net force and moment zero. In particular there is an instantaneous translational velocity $(\dot{(X)}, \dot{Y}, \dot{Z})$.

We are interested in cases of motion in the standard frame in which steady locomotion is not possible. We shall assume that the standard movement is periodic with period T, so that the configuration path is closed. Suppose now that the path P in configuration space is indistinguishable from the path P' which results from the replacement of t by $-t$, in other

---

[3]The non-singular property of $\mathbf{A}$ or $\mathbf{B}$ follows from the fact that any rigid body motion produces non-trivial viscous dissipation.

words from the sequence of configurations obtained by running the parameter clock backwards. We call such a periodic movement a *reciprocal movement*.

To take a discrete case, if $P = ABCDEFGA$, $P' = AGFEDCBA$ and $P = P'$ if and only if $P = ABCDDCBA$. For continuous movements, a reciprocal path must go from the starting configuration, A say, along a curve C connecting A to an intermediate configuration $B \neq A$, then back along the curve $-C$ from B to A. We might say that a reciprocal movement may be characterized as a union of degenerate oriented loops segments such as AB in Figure 2.1(a), which are "twice covered" and hence invariant under time reversal. A non-reciprocal movement will be non-degenerate in the sense that some component will be "once-covered" and hence not invariant under time reversal. To identify non-reciprocity it suffices to show the existence of a once-covered segment on some low-dimensional projection of the configuration space.

For example, consider the stretched plane sheet, with $x_B(x,t) = x + a\cos(kx - \omega t)$. Consider the 2D con figuration space consisting of

$$c_1(t) = x_B(0,t) = a\cos\omega t, c_2 = x_B(\pi/(2k), t) = \pi/(2k)\sin\omega t. \quad (2.34)$$

This 2D projection of the configuration space (fully determined by the movements of the points $0 \leq x < 2\pi$ say) yields an oriented circle, so that the motion of the sheet is non-reciprocal. The impications of time-reversal symmetry should be carefully considered in the light of this example.It is not simply a matter of material orbits of boundary points being indistinguishable from their time reversals. That occurs in the above example, where the relative phase of distinct boundary points must be invoked to see that the movement is not reciprocal. In a sense one must consider the entire collection of boundary points in tracking the time evolution of the body configuration.
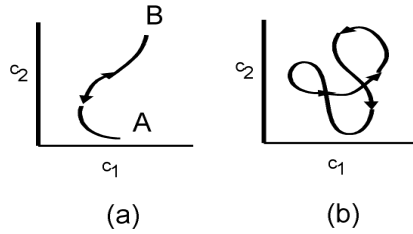

Figure 2.1: Movements which are (a)reciprocal and (b) non-reciprocal in a 2D configurations space of parameters c_1, c_2.

We now state a fundamental result of Stokesian locomotion: *If the standard movement of a periodic Stokesian locomoter is reciprocal, steady locomotion with non-zero velocity is not possible.* This might be termed the *reciprocal theorem*, but it is usually called the *scallop theorem*, see the delightful lecture of Purcell [12].

The proof of the scallop theorem depends on linearity and the reversal of the sign of velocity under time reversal. This is true for the standard shape, as well as for the current shape since there is a one-one correspondence of the rigid-body motion and the standard velocity. Over a given period it follows that, if the translational displacement of the body over one period is $\Delta \mathbf{X}$, the displacement over one period with time-reversed motion is $-\Delta \mathbf{X}$. If the motion is reciprocal, the two movements are indistinguishable, so that $\Delta \mathbf{X} = -\Delta \mathbf{X}$, so there is not displacement.

Note that we are dealing here only with net displacements over one period. In general a body will move during the cycle, as in the back and forth movement of a scallop shell when trying to swim in the Stokesian realm.

Note also that the scallop theorem does *not* say that a non-reciprocal movement necessarily results in locomotion. Indeed it is easy to come up with counter-examples, where two components of the movement are each non-reciprocal, but their effects cancel (e.g. two flagella acting on a cell body from opposite directions).

We remark that there are generalizations of the scallop theorem which depend upon symmetries of the Stokes equations. For example, the mirror image of a Stokes for is a Stokes flow. As a consequence, if the mirror image of a body movement is indistinguishable from the time reversed movement, Stokesian swimming is impossible. An example of this would be a rigid stalk pivoting about one end and sweeping a circular conical surface.

2.5   Efficiency of Stokesian locomotion

Consider a neutrally buoyant body in steady locomotion with mean velocity $\mathbf{U}$. With respect to an observer moving with the velocity $\mathbf{U}$, the fluid velocity exterior to the body may be decomposed as follows:

$$\mathbf{u} = -\mathbf{U} + \mathbf{u}_1 + \mathbf{u}_2, \qquad (2.35)$$

where $\mathbf{u}_1$ is the Stokes flow vanishing at ∞ and equal to $\mathbf{U}$ on the instantaneous body surface, and $\mathbf{u}_2$ also vanishes at ∞ and is equal to one the body surface to the instantaneous body velocity $\mathbf{u}_B$. Note that the motion of the body surface relative to the observed in uniform motion is in general *not* that observed in the standard frame. This is because the translational velocity of the body is in general a function of time with time average $\mathbf{U}$.

The force exerted on the fluid by the body movements is

$$\mathbf{F}_2(t) = -\int \sigma_2 \cdot \mathbf{n} dS, \qquad (2.36)$$

the integral being over the instantaneous body surface with outward normal $\mathbf{n}$. This force satisfies $\mathbf{F}_2(t) = -\mathbf{F}_1(t)$, where $\mathbf{F}_1$ is the force exerted by the instantaneous body surface being moved with velocity $\mathbf{U}$.

We now define the efficiency η of locomotion as the time average of the rate of working of $\mathbf{F}_2$ during locomotion, divided by the time average of the total viscous dissipation of the flow,

$$\eta = \frac{\langle \mathbf{F}_2 \cdot \mathbf{U} \rangle}{\langle \Phi \rangle} = \frac{\langle \mathbf{F}_2 \rangle \cdot \mathbf{U}}{\langle \Phi \rangle} = \frac{-\langle \mathbf{F}_1 \rangle \cdot \mathbf{U}}{\langle \Phi \rangle}, \tag{2.37}$$

where $\langle \cdot \rangle$ denotes time average and Φ is the dissipation of $\mathbf{u}_1 + \mathbf{u}_2$. But

$$\langle \mathbf{F}_1 \rangle \cdot \mathbf{U} = \langle \int \mathbf{U} \cdot \sigma_1 \cdot \mathbf{n} dS \rangle = \langle \int \mathbf{u}_1 \cdot \sigma_1 \cdot \mathbf{n} dS \rangle \tag{2.38}$$

Taking into account the normal is *outward* from the body, we see that

$$\langle \mathbf{F}_1 \rangle \cdot \mathbf{U} = -\langle \Phi_{11} \rangle, \tag{2.39}$$

where we write

$$\Phi_{kl} = \frac{\mu}{2} \int \left(\frac{\partial u_{ki}}{\partial x_j} + \frac{\partial u_{kj}}{\partial x_i} \right) \left(\frac{\partial u_{li}}{\partial x_j} + \frac{\partial u_{lj}}{\partial x_i} \right) dV, \tag{2.40}$$

taken over the exterior domain. We may show in a similar way, using $\mathbf{F}_1 + \mathbf{F}_2 = 0$, that

$$\langle \Phi_{21} \rangle = -\langle \Phi_{11} \rangle. \tag{2.41}$$

Thus we have

$$\eta = \frac{\langle \Phi_{11} \rangle}{\langle \Phi_{11} + 2\Phi_{12} + \Phi_{22} \rangle} = \frac{\langle \Phi_{11} \rangle}{\langle \Phi_{22} \rangle - \langle \Phi_{11} \rangle}. \tag{2.42}$$

2.6   The general half-plane problem: the swimming of a sheet reconsidered

The problem of a swimming sheet may be generalized to allow the sheet to both undulate in the y direction, and it so doing to stretch slightly, but also to directly stretch along its surface. Accordingly we consider the boundary motion

$$x_B = x + a \cos(kx - \omega t - \phi)$$
$$= x + \beta \cos \xi + \gamma \sin \xi, \ \xi = kx - \omega t, \tag{2.43}$$
$$y_B = b \sin \xi, \tag{2.44}$$

where $\beta = a \cos \phi, \gamma = a \sin \phi$. The analysis proceeds exactly as for the stretched, planar sheet, using the modified boundary conditions at the sheet:

$$u(x_B, y_B, t) = a\omega \sin(\xi - \phi) \tag{2.45}$$

$$v(x_B, y_B, t) = -b\omega \cos \xi. \tag{2.46}$$

For small ak, bk, the first two terms in the expansion of the streamfunction (with $xi = kx - \omega t$band $\eta = ky$) are found to be

$$\psi_1 = \frac{\omega}{k}[(b + b\eta + \beta\eta)e_{-\eta} \sin \xi - \gamma\eta e^{-\eta} \cos \xi], \tag{2.47}$$

$$\psi_2 = Uy - \frac{\omega}{2}\eta e^{-2\eta}[2\gamma(b + \beta) \sin 2\xi + (b + \beta + \gamma(b + \beta - \gamma) \cos 2\xi]. \tag{2.48}$$

Here leading term U_2 of the expansion of the swimming speed is again of order $(ak)^2 \sim (bk)^2$, and is given by

$$U/V = \frac{1}{2}k^2(b^2 + 2ab \cos \phi - a^2), \; V = \omega/k. \tag{2.49}$$

Note that the direction of swimming opposed to the phase velocity of the wave when $a = 0$, but as we have seen is in the direction of the wave when $b = 0$. This is a consequence of the differing effect on the fluid of undulating as opposed tangential movements. We shall see the same phenomena in locomotion by waving flagella, where the effect is direction of swimming relative to the phase speed is determined by the relative resistance of the flagellum to movements along its axis as opposed to normal to its axis.

We may interpret the swimming as an average property of the sheet's waviness. If the fluid were initially at rest and the waves were started, the flow would build up with time until a bulk motion of the fluid "at infinity" had developed. A precise mechanical desription of the origin of this bulk motion is difficult to give because it is a second-order effect. Intuitively, it is not surprising that bulk motion can be developed in a viscous fluid, but even its directiion is difficulty to predict from the sheet's parameters.

2.6.1   Other results

The pressure field corresponding to ψ may be found from the formula

$$\frac{\partial p}{\partial x} = \mu\nabla^2\frac{\partial\psi}{\partial y}, \tag{2.50}$$

because the right-hand side is periodic in x with zero mean. To leading order we find,

$$p_1 = -2\mu\omega ke^{-\eta}[(b + \beta) \cos \xi + \gamma \sin \xi]. \tag{2.51}$$

Despite the fact that the sheet does not swim to leading order, the effort or mechanical work done by the sheet while swimming can be computed from the leading terms. The work done by the sheet, per unit horizontal projected area, is

$$W_s = -\langle u(x_B, y_B, t)(\sigma_{11}n_1 + \sigma_{12}n_2) + v(x_B, y_B, t)(\sigma_{21}n_1 + \sigma_{22}n_2)\rangle, \tag{2.52}$$

where $n_1(x,t), n_2(x,t)$ is the upward normal vector from the sheet,

$$n_1 = -\Delta(1+\delta^2)^{-1/2}, n_2 = (1+\Delta)^{-1/2}, \Delta = \frac{dy_B}{dx} = bk\cos\xi, \quad (2.53)$$

and

$$\sigma = \begin{pmatrix} -p + 2\mu\psi_{xy} & \mu(\psi_{yy} - \Psi_{xx}) \\ \mu(\psi_{yy} - \Psi_{xx}) & -p - \mu\psi_{xy} \end{pmatrix}. \quad (2.54)$$

From these expressions we may calculate

$$W_s = \mu\omega^2 k(a^2 + b^2). \quad (2.55)$$

This value is to be doubled if both sides of the sheet are considered.

Some other quantities of interest in applications of the swimming sheet are the constant *fluxes* of mass and momentum associated with its movements. let f_m, f_x, f_y denote fluxes of mass and (x,y) momentum. Then

$$f_m = -\langle\psi(x,y_B,t) - Uy_B\rangle$$

$$\sim -\langle\psi_1(x,y_B,t)\rangle = -\frac{1}{2}\beta b. \quad (2.56)$$

Similarly, using (2.54) we have

$$f_x = \langle\int_{y_B}^\infty \sigma_{11}dy\rangle = -2\mu\omega k\gamma b, \quad (2.57)$$

$$f_y = \langle\int_{y_B}^\infty \sigma_{21}dy\rangle = \mu\omega k\beta b. \quad (2.58)$$

These fluxes can affect the flow field whenever the parameters of the sheet are slowly modulated in space, see the macroscopic model of section ??.

Finally, wegive the finite Reynolds number result for U in the case $a = 0$, obtained exactly as for the case $b = 0$.

$$U/V = \frac{b^2 k^2}{4}\left(1 + \frac{1}{F}\right). \quad (2.59)$$

Thus in this case the speed is decreased by one-half as the Reynolds number increases from zero to infinity.

2.6.2   Inextensibility

In [14] G.I. Taylor actually focuses on the case $b = 0$ with the sheet assumed to be *inextensible*, i.e to preserve arc length during its motion. Relative to the *stationary* frame in which the points of the sheet are seen to execute periodic orbits, assume that the phase velocity of the wave is positive, so the wave move to the right. Changed now to a *moving* frame, moving with the phase velocity of with wave, the standing wave of crests and troughs

is seen to be fixed in space, but material points on the sheet are observed to be moving to the left. Moreover, the sheet being inextensible, the *speed* of this motion of material points within the sheet must be the same for all points, equal say to Q. During the time the stationary observed sees one wave length of the wave pass by, material points must move along the full arc length of one wavelength of the surface. Thus

$$Q = \frac{V \times arc\ length\ of\ one\ wavelength\ of\ sheet}{one\ wavelength\ of\ wave}, \qquad (2.60)$$

and so,

$$Q = \frac{\omega}{2\pi k} \int_0^{2\pi} (1 + b^2 k^2 \cos^2 \xi) d\xi. \qquad (2.61)$$

The stationary observed thus sees the boundary velocity

$$u(x_B, y_B, t) = -Q \cos \theta + V, v(x_B, y_B, t) = -Q \sin \theta, \qquad (2.62)$$

where $\tan \theta = dy_b/dx = bk \cos \xi$. Substituting (2.61) and expanding, we get

$$u(x_B, y_B, t) = \frac{\omega b^2 k}{4} \cos 2\xi + O(b^4 k^4), \qquad (2.63)$$

$$v(x_B, y_B, t) = -b\omega \cos \xi + O(b^3 k^3). \qquad (2.64)$$

For small bk a material is seen by the stationary observer to have Lagrange coordinates

$$(x_B, y_B) = (x - \frac{1}{8} b^2 k \sin 2\xi, b \sin \xi). \qquad (2.65)$$

This shows that material points execute small figure eights relative to the stationary observer. It follows also from this that the sheet movement is non-reciprocal.

Taylor carried his calculation of U with inextensibility assumed to order $b^4 k^4$, finding

$$U/V = \frac{1}{2} b^2 k^2 (1 - \frac{19}{16} b^2 k^2) + O(b^6 k^6). \qquad (2.66)$$

2.7   Flagellar locomotion

Although the swimming sheet will provide a useful model of ciliary propulsion (see ??), it is not in itself representative of a natural organelle for low Reynolds number locomotion. By far the most common strategy seen in nature is to utilize long slender organelles, such as cilia, flagella, and rigid stalks as the building material for a locomoting body. We shall attempt in this section to understand the usefulness of this body geometry from the mechanical principles of Stokesian fluid dynamics.

2.7.1 Approximate theory for a thin stalk

Since a long slender filament in Stokes flow can presumably apply force
to the fluid, forces necessarily concentrated near a curve, it is tempting
to represent its hydrodynamical effect in terms of a distribution of tensor
Stokeslets,

$$S_{ij}(x,y,z) = \frac{1}{8\pi\mu}\left(\frac{x_i x_j}{r^3} + \frac{1}{r}\delta_{ij}\right). \tag{2.67}$$

Let us consider for simplicity a straight stalk whose axis lies along the
segment $-L_1 \le z \le L_2$ of the z-axis, and let the boundary of the stalk be
the cylinder $x^2 + y^2 = a^2, -L_1 \le z \le L_2$. We assume that $a \ll L_1 + L_2$.

Our object now is a see what surface velocities result from a *given* distri-
bution of forces along the axis of the stalk, and try to adjust the forces so
that the surface velocity amounts to a rigid-body motion of the stalk. If we
succeed, the superposition of Stokeslets represents the Stokes flow created
by the motion of the stalk.

Let $\mathbf{f}_t(\zeta)\delta(x)\delta(y\delta(z-\zeta)$ be the tangential force at the axis of the stalk,
and $\mathbf{f}_n(\zeta)\delta(x)\delta(y\delta(z-\zeta)$ be the force normal to the stalk, both at the point
$z = \zeta$. Here $\mathbf{f}_t = (f_z(\zeta),0,0)$ and $\mathbf{f}_n = (f_x(\zeta), f_y(\zeta),0)$. We seek to evaluate
in the neighborhood of the stalk surface the integrals

$$(\mathbf{u}_t, \mathbf{u}_n = \int_{-L_1}^{L_2} \mathbf{S}(x,y,z-\zeta)\cdot(\mathbf{f}_t, \mathbf{f}_n)d\zeta \tag{2.68}$$

We will show, following Lighthill [17] that a useful approximate theory can
be developed by first taking the force distribution as a constant.

We note the following indefinite integrals:

$$\int \left(\frac{z^2}{r^3} + \frac{1}{r}\right)dz = -z/r + 2\log(z+r), \tag{2.69}$$

$$\int z(x,y)/r^3 dx = -(x,y)/r. \tag{2.70}$$

Thus if $\mathbf{f}_t \ne 0$ were independent of ζ, we would have

$$8\pi\mu f_z^{-1}w_t = \int_{-L_1}^{L_2} \frac{(z-\zeta)^2}{(x^2+y^2+(z-\zeta)^2)^{3/2}} + \frac{1}{(x^2+y^2+(z-\zeta)^2)^{1/2}}d\zeta$$

$$= \frac{(z-L_2)}{(x^2+y^2+(z-L_2)^2)^{1/2}} - \frac{(z+L_1)}{(x^2+y^2+(z+L_1)^2)^{1/2}}$$

$$-2\log\left(\frac{z-L_2+\sqrt{x^2+y^2+(z-L_2)^2}}{z+L_1+\sqrt{x^2+y^2+(z+L_1)^2}}\right) \tag{2.71}$$

These terms not involving the logarithm have an interesting structure when
$z^2 + y^2 = a^2$ and z varies from $-L_1$ to L_2. We show graphs in Figure 2.2
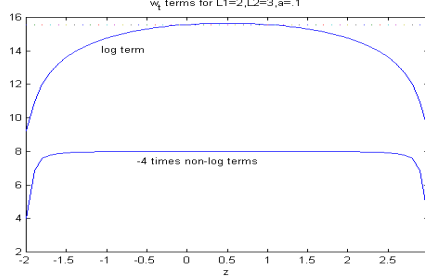
Figure 2.2: The terms in w_t for the case $L_1 = 2, L_2 = 3, a = .1$. The dotted line is $2\log(2400)$.

The logarithmic terms clearly are not well approximated by a constant, but that is nevertheless the approximation usually made. In fact the dominant terms in the expansion for small a^2 where z is bounded away from the endpoints of the stalk are adopted:

$$w_t = f_z \frac{1}{4\pi\mu}\Big[\log\big(\frac{4L_1L_2}{a^2}\big) - 1\Big]f_z + O(a^2 L^{-2}), L = (L_1L_2)^{1/2}. \quad (2.72)$$

We also have on $x^2 + y^2 = a^2$,

$$8\pi\mu f_z^{-1}(u_t, v_t) = (x, y)[(a^2 + (z - L_2)^2)^{-1} - (a^2 + (z + L_1)^2)^{-1}]. \quad (2.73)$$

Thus, away from the endpoints we have $(u_t, v_t) = O(a/L)$. Thus, in leading terms

$$\mathbf{u}_t = \frac{1}{4\pi\mu}\Big[\log\big(\frac{4L_1L_2}{a^2}\big) - 1\Big] + \mathbf{f}_t + O(a/L). \quad (2.74)$$

Consider now the effect of the x-directed point forces. Again assuming f_x is independent of ζ. The resulting velocity is

$$8\pi\mu f_x^{-1}\mathbf{u}_n = \int_{-L_1}^{L_2} \frac{(2x^2 + y^2 + (z - \zeta)^2, xy, x(z - \zeta))}{(x^2 + y^2 + (z - \zeta)^2)^{3/2}}d\zeta. \quad (2.75)$$

We now need to use, in addition to (2.69), (2.70)

$$\int r^{-3}dz = \frac{z}{(x^2 + y^2)r}, \quad (2.76)$$

$$\int r^{-5}dz = \frac{z}{3a^2r^3} + \frac{2z}{3a^4r}. \quad (2.77)$$

We then find, away from endpoints, that on $x^2 + y^2 = z^2$ we have

$$8\pi\mu f_x^{-1}\mathbf{u}_n = \big(\frac{2x^2}{a^2} + \log\frac{4L_1L_2}{a^2}, \frac{2xy}{a^2}, 0\big) + O(a/L). \quad (2.78)$$

The terms here in x^2 and xy are formally O(1) and need to be dealt with. We therefore consider a potential flow contribution to the Stokes flow, given by dipole velocity $\nabla(x/r^3)$. The velocity field for this dipole is

$$(r^{-3} - 3x^2 r^{-5}, -3xy r^{-5}, -3xz r^{-5}). \tag{2.79}$$

If we assume a uniform distribution of strength g over the stalk, the resulting flow, when evaluated on the stalk, takes the form

$$\mathbf{u}_g = g\Big(\frac{2}{a^2} - \frac{4x^2}{a^4}, \frac{-4xy}{a^4}, 0\Big) + O(a/L). \tag{2.80}$$

Now choosing $g = \frac{a^2}{16\pi\mu}$ and combining the two fields, we obtain a composite $\mathbf{u}_n$ given by

$$\mathbf{u}_n = \frac{1}{8\pi\mu}\Big[\log\big(\frac{4L_1 L_2}{a^2}\big) + 1\Big]\mathbf{f}_n + O(a/L), \tag{2.81}$$

where we now include the contribution of f_y as obtained by a parallel computation.

We can turn the relation between force and velocity around, and view (2.74) and (2.81) as relations defining a *resistance* to motion of the stalk in the tangential and normal directions respectively. Strictly speaking the resistance so calculated is exact only in the limit of zero a, and the logarithmic terms are such as to make the expressions convergence very slowly to this limit. Nevertheless, these results have led to the use of an approximate way of studying the resistance of a slender, flexible flagellum of arbitrary shape to tangential and normal movements. The idea is to introduce tangential and normal *resistance coefficients* K_T, K_N, so that $u_t K_T \Delta s$ and $u_n K_N \Delta s$ are respectively the tangential and normal forces exerted on the fluid by a small segment of flagellum of length Δs, in motion through the fluid with tangential and normal velocity u_t, u_n. If a is the radius of the cross section of the flagellum, then the force is intended to be calculated for a slender object, so necessarily $\Delta s \gg a$.

In first glance it would seem that we have already, in (2.74) and (2.81), a nice approximate derivation of K_T, K_N. Note that (2.74) and (2.81) suggest that , because of critical factor of 2, when the logarithm dominates we can expect K_N to be about twice K_T. In practice the factor is smaller, but K_N/K_T may be safely assumed to exceed 1 for any slender smooth flagellum. However there is a basic problem in the use of these formulas. The expressions involve the product bc, and it is unclear what value should be assigned to this constant. Various ways of dealing with this calibration problem have been proposed, and we will return to it when we take up the more formal theory in section ??. For now we simply adopt the the very useful premise that suitable K_T, K_N can be found, and proceed to construct a theory of flagellar propulsion. We shall see later that in fact a purely local theory of flagellar resistance is not mathematically tenable, so

the method is leads to a simple, transparent model rather than an exact asymptotic formulation.

2.7.2   Gray-Hancock theory of flagellar propulsion

This theory studies the motion of a flagellum idealized as a curve in space whose motion through the fluid leads to forces derivable from resistance coefficients. The theory, due to Gray and Hancock [19], is is a *resistive force theory.*

We represent the instantaneous position of the flagellum in terms of its arc length,

$$\mathbf{r} = (x, y, z) = \mathbf{R}(s) = \big(X(s), Y(s), Z(s)\big). \tag{2.82}$$

Then $d\mathbf{R}/ds = \mathbf{t}$ is the local tangent vector in the direction of increasing s. We assume the wave form to be periodic and the motion to be along the x-axis, so that there are constants Λ, λ such that

$$X(s + \Lambda) = X(s) + \lambda, Y(s + \Lambda) = Y(s), Z(s + \Lambda)) = Z(s). \tag{2.83}$$

Thus Λ is the distance along the length of the curve needed to travel one wavelength λ along the x-axis:

$$\alpha = \frac{\lambda}{\Lambda} = \frac{wavelength}{arc\ length\ of\ one\ wave}. \tag{2.84}$$

Thusα^{-1} is the expansion factor for arc length accounting for waviness.

We assume that the flagellum is inextensible. As in the swimming inextensible sheet, an observer moving to the right who sees a standing wave, will see a point of the flagellum moving along the sheet to the left. Because of inextensibility, the speed of the point is a constant Q, the velocity along the flagellum being $-Q\mathbf{t}$. We then have,

$$V = \alpha Q. \tag{2.85}$$

The observer watching a standing wave thus sees the material points as satisfying

$$\mathbf{r} = \mathbf{R}(s + Qt). \tag{2.86}$$

If now the flagellum swims with velocity $U\mathbf{i}$, a material point on the flagellum moves relative to the fluid at infinity with velocity $\mathbf{w}$, where

$$\mathbf{w} = (U + V)\mathbf{i} - Q\mathbf{t}. \tag{2.87}$$

At this stage the fundamental assumption of resistive force theory is made. If K_T, K_N are the flagellar resistance coefficients discussed above, it follows that $\mathbf{w} \cdot (K_T\mathbf{t} + K_N\mathbf{n})ds$ is the force $d\mathbf{F}$ exerted on the fluid by a length ds of flagellum at a point with tangent and normal vectors $\mathbf{t}, \mathbf{n}$. The total

force $\mathbf{F}$ exerted on the fluid by on a length L of flagellum may then be written in a form which avoids reference to the normal vector explicitly,

$$\mathbf{F} = \int_0^L \mathbf{w} \cdot \mathbf{M} ds, \; \mathbf{M} = (K_T - K_N)\frac{d\mathbf{R}}{ds}\frac{d\mathbf{R}}{ds} + K_N \mathbf{I}. \tag{2.88}$$

Using (2.86) in (2.88) we obtain the total thrust T exerted by the flagellum on the fluid

$$T = \mathbf{F} \cdot \mathbf{i} = (K_T - K_N)(U+V)\int_0^L (X')^2 ds + K_N(U+V)L - K_T Q \int_0^L X' ds. \tag{2.89}$$

Defining β by

$$\int_0^L (X')^2 ds = \beta L, \tag{2.90}$$

and noting that

$$\int_0^L X' ds = \alpha L = \frac{VL}{Q}, \tag{2.91}$$

we obtain

$$T = (V + U)[(K_T - K_N)\beta L + K_N L] - K_T V L. \tag{2.92}$$

We can now study how the flagellum can swim. If the organism consists only of flagellum, necessarily U is found by setting T as given by (2.92) equal to zero. This defines the *zero thrust swimming velocity U_0*;

$$\frac{U_0}{V} = \frac{(\rho - 1)(1 - \beta)}{\rho\beta + 1 - \beta}, \; \rho = \frac{K_T}{K_N}. \tag{2.93}$$

Since $\beta < 1$, we see that $U_0/V < 0$ if $\rho < 1$, so that the swimming is opposite to the phase velocity of the wave when the flagellum exerts greater normal than tangential force. The calculations of resistance based upon local theory indicated that $.5 < \rho < 1$ so that smooth flagella should always swim in a direction opposite the phase velocity of the wave.

If the flagellum is attached to a head, the thrust developed by the tail must balance the extra drag of the head, and which we take to be $LUK_N\delta$. Then swimming spped U is less than U_0, i.e. the flagellum drifts backward relative to the zero thrust swimming seed. Thus we may write

$$LUK_N\delta = (V + U)[(K_T - K_N)\beta L + K_N L] - K_T V L, \tag{2.94}$$

and therefore

$$LUK_N\delta = (U - U_0)[(K_T - K_N)\beta L + K_N L], \tag{2.95}$$

It follows that $(K_T - K_N)\beta + K_N$ is a composite resistance for the flagellum as a whole, the waveform information being only in the parameter β.

With the head attached, (2.93) thus becomes

$$\frac{U_0}{V} = \frac{(\rho - 1)(1 - \beta)}{\rho\beta + 1 - \beta + \delta}.$$ (2.96)

In calculating δ, it is usually acceptable to neglect the interaction of the head with the tail, given that the tail is very slender.

Helical waves

Helical flagellar waves result from superposition of two orthogonal planar waves, so that, relative to the moving observer seeing backwards tangential motion along the flagellum,

$$\mathbf{R}(s) = \big(\alpha(s + Qt), b\cos k(s + Qt), b\sin k(s + Qt)\big).$$ (2.97)

Here as before αQ is the phase speed V, and $\alpha^2 + b^2 k^2 = 1$ by the definition of s. Shifting back to the stationary observer, the velocity of a material point on the flagellum is

$$(dX/dt - V, dY/dt, dZ/dt) = \big(0, -bk\sin k(s + Qt), bk\cos(k(s + Qt))\big), (2.98)$$

and is therefore equivalent to a rigid rotation of the helical structure about its axis.

We have so far discussed only thrust, but helical waves bring up explicitly the matter of the balance of torques in flagellar hydrodynamics. Within Gray-Hancock theory the torque balance may be computed from the moments of resistance forces, but there is in addition the question of rotation of the flagellum. If the flagellum is regarding as a rigid structure, it will rotate along with the helical wave. If on the other hand the surface of the flagellum is not free to rotate with the wave, torques associated with the finite cross section of the flagellum can be eliminated.[4]

We remark that within Gray-Hancock theory, simultaneous torque and thrust balance for a headless flagellum is impossible, see exercise 2.5. Head rotation, as well as restoring torques due to the mass distribution in a gravitational field, can provide the balance. An appealing idea, due to Chwang and Wu [5], is to use rotation of the flagellum itself to balance swimming torque. A circular cylinder of radius a spinning on its axis with angular velocity Ω in a viscous fluid generates a simple steady velocity field

$$\mathbf{u} = \frac{a^2 \Omega \times \mathbf{r}}{r^2},$$ (2.99)

where r is the cylindrical polar radius. The resulting torque on the fluid per unit length is $2\pi\mu a^2\Omega$. For a curve of projected length αL, the net torque

---

[4]G.I. Taylor [15], in a delightful experiment, constructed a device with zero flagellum torque by rotating a rigid helical wire inside of a flexible tube, the tube being fixed to an essentially stationary body.

about the line of swimming is $2\pi\mu a^2 \Omega L \alpha$, and this is available for canceling the sswimming torque. The body rotation does not affect (to leading order) the thrust and moment caculations of resistive force theory.

Efficiencies in resistive force theory

It is of interest to examine the efficiency of flagellar locomotion in the context of Gray-Hancock theory, because the rather simple expressions allow an investigation of the effect of body geometry as well as various ways to define efficiency

Efficiency should be a the ratio of the absolute minimum work needed to locomote the body at some speed, divided by the work acually done to locomote the body at that speed. In Stokes flow and for the same body, different motions relative to the standard frame would in general lead to different efficiencies of locomotion.

According to Gray-Hancock theory, the total work done by the flagellum is just

$$\int_0^L \mathbf{w}\cdot\mathbf{F}ds = \int_0^L \mathbf{w}\cdot\mathbf{M}\cdot\mathbf{w}ds = \int_0^L [(\mathbf{w}\cdot\mathbf{t})^2(K_T-K_N)+K_N w^2]ds. \quad (2.100)$$

Inserting (2.87) we obtain

$$\text{Work} = \Phi = K_T L[(V+U)^2\beta - 2V(V+U) + Q^2] + K_N L(U+V)^2(1-\beta). \quad (2.101)$$

Since we know total work equals total viscous dissipation, we have recalled the symbol Φ which we have used for the latter, and dropped the time average as irrelevant to the present calculations.

Using the definitions (2.40) in our previous discussion of efficiency, it is of interest to consider the decomposition $\Phi = \Phi_{11} + 2\Phi_{12} + \Phi_{22}$ in the context of a resistive force theory. Now we have noted from (2.95) that the effective resistance coefficient for the flagellum is $(K_T - K_N)\beta + K_N$, so that Φ_{11} will equal the work done by moving an object with this resistance coefficient at the swimming speed U. Recalling that Φ_{22} was defined only in terms of body movements while swimming, in Gray-Hancock theory it must equal to the work done if the swimming speed is *zero*. Thus

$$\Phi_{11} = U^2 L[(K_T - K_N)\beta + K_N], \quad (2.102)$$

$$\Phi_{22} = V^2 K_T L(\beta - 2 + \alpha^{-2}) + V^2 K_N L(1-\beta), \quad (2.103)$$

and so

$$\Phi_{12} = VU(K_T - K_N)L(\beta - 1). \quad (2.104)$$

Notice that, if U is equal to the zero thrust swimming speed, so that $U[(K_T - K_N)\beta L + K_N L] = V(K_T - K_N)(1 - \beta)L$, then $\Phi_{11} = -\Phi 12$ as was noted to follow from our general arguments.

If we now adopt the efficiency (2.42), we may write this as

$$\eta = (\Phi_{22}/\Phi_{11} - 1)^{-1}, \tag{2.105}$$

so that the efficiency is maximized by minimizing Φ_{22}/Φ_{11}. Now by the Schwarz inequality it follows that $\alpha^2 \leq \beta$, and therefore to maximize efficiency we takin $\alpha^2 = \beta$ in Φ_{22}. Then, in zero thrust swimming, we have

$$\Phi_{22}/\Phi_{11} \geq \frac{[K_T - (K_T - K_N)\beta][(K_T - K_N)\beta + K_N]}{(K_T - K_N)^2(1 - \beta)\beta}, \tag{2.106}$$

or

$$\Phi_{22}/\Phi_{11} \geq \frac{[\rho - (\rho - 1)\beta][(\rho - 1)\beta + 1]}{(\rho - 1)^2(1 - \beta)\beta}. \tag{2.107}$$

Note that any extremum of this ratio is also an extremum of $1/\beta + \beta/(1-\beta)$. Thus we obtain a minimum at $\beta = 1/2$, so that

$$\Phi_{22}/\Phi_{11} \geq (1 + \rho)^2/(1 - \rho)^2. \tag{2.108}$$

The maximum efficient is thus

$$\eta_{max} = \frac{(1 - \rho)^2}{4\rho}, \tag{2.109}$$

occuring with $U_0/V = \frac{\rho-1}{\rho+1}$. A reasonable choice of ρ is .7, yielding $\eta_{max} = .032$ and $U_0/V = -.176$. These numbers are typical are typical of Stokesian swimming.

Other definitions of efficiency have been used. Lighthill [17] introduces an efficiency for the headless flagellum $K_T L U^2 L/\Phi$. That is, the work done by the tangential drag of the *stretched straight* flagellum is divided by total dissipation. This differs from (2.42) only in that the drag is for the stretched straight rather than the wavy body. We can therefore expect this efficiency to be lower than (2.42). Again maximizing with respect to $\beta = \alpha^2$, the optimal β is found to be $(1 + \rho^{1/2})^{-1}$ and there results

$$\eta_{max} = (1 - \rho^{1/2})^2, U_0/V = \rho^{1/2} - 1. \tag{2.110}$$

With $\rho = .7$ we then have $\eta_{max} = .027, U_0/V = -.163$.

If the wave is helical with $\beta = \cos^2 \psi$ where ψ is the pitch angle of the helix, then Lighthill's op[timal efficiency at $\rho = .7$ gives an optimal pitch angle of 42°, while (**??**) gives 45°.

Both of these efficiencies can exceed unity for sufficiently large ρ, namely $\rho > 0$ for (2.110) and 5.83 for (2.42). We shall see in the next section that such values lie way beyond the numbers predicted by asymptotic theories of flagellar hydrodynamics. Of course we are dealing here with an approximate Stokesian theory based upon resistance force theory. Nevertheless it is reasonable to propose that η as defined by (2.42) cannot exceed unity, implying the general result $\Phi_{11} \leq \frac{1}{2}\Phi_{22}$.

2.8   Formal theory of slender bodies

Batchelor [3], and Cox [4] have shown that Stokes flow past slender bodies of characteristic length L and radius of cross section a can, for small $\epsilon = a/L$, be expressed expressed as an asymptotic expansion in powers of $[-\log(\epsilon/2)]^{-1}$. Although these studies are of fundamental importance for the motion of slender bodies in Stokes flow, this asymptotic expansion is not well adapted to the study of zero-thrust swimming. This point was made by Lighthill [18], who notes that for a zero-thrust flagellum there is considerable advantage in using a the approach of the loical theory given above, by asking for *the boundary compatible with a given force-dipole distribution*, rather than the other way around, where the body is moved and we fond the required force-dipole distribution. Lighthill formulates this approach in terms of a key theorem which we now present and prove with the help of elementary estimates.

We again consider a flagellum having a circular cross section of constant radius a, and having as axis a curve $\mathcal{C} : \mathbf{r} = \mathbf{R}(s)$. By Stokeslet we again mean the field (2.67), and by dipole with moment $\mathbf{i}$ we mean the field $\frac{1}{4\pi}\nabla(x/r^3)$.

Theorem 1 *Let $\mathbf{u}$ be the flow field consisting of a Stokeslet distribution of strength $\mathbf{f}(s)$ on C, plus a dipole distribiution of moment $-a^2\mathbf{f}_n/4\mu$ on $\mathcal{C}$, where $\mathbf{f}_n(s)$ is the projection of $\mathbf{f}$ onto the plane $\mathcal{P}(s)$ perpendicular to $\mathcal{C}$. Consider z section $s = s_0$ and let $\sigma(s_0)$ denote the circular intersection of $\mathcal{P}(s_0)$ with the surface of the flagellum. We assume*
(1) that the improper integral of Stokeslets $\mathbf{S}$,

$$\int_{|s-s_0|>A} \mathbf{S}(\mathbf{r} - \mathbf{R}(s)) \cdot \mathbf{f}(s)ds \qquad (2.111)$$

defines a function of $\mathbf{r}$, differentiable in some neighborhood of the center of σ_0 for each $A > 0$;
(2)that $\mathbf{f}'(s)$ and $\mathbf{R}''(s)$ are continuous function, uniformly for $-\infty < s < +\infty$;
(3) that there is a constant B such that $|\mathbf{R}(s) - r_0| > B|s - s_0|$ for sufficiently large $|s-s_0|$, where $\mathbf{r}_0$ is the position vector for the point $s = s_0$.
Let

$$f_0 = \max_s |\mathbf{f}(s)|, L^{-1} = \max_s |\mathbf{R}''(s)|, l^{-1} = f_0^{-1} \max_s |\mathbf{f}'(s)|, \qquad (2.112)$$

and set $\epsilon = a/L$. Then, as $\epsilon \to 0$,

$$\mathbf{u}(\sigma_0) = \frac{1}{4\pi\mu}\mathbf{f}_n(s_0) + \int_{|\mathbf{r}_0-\mathbf{R}|>\delta} > \delta\mathbf{S}(\mathbf{r}_0 - \mathbf{R}(s)) \cdot \mathbf{f}(s)ds + O(E), \ (2.113)$$

where $\delta = \frac{a\sqrt{e}}{2}$ and $E = (f_0/\mu)(1 + L/l)\epsilon^{1/2}$.[5]

---

[5]Here as well as elsewhere we use the $O(\cdot)$ symbol in its technical sense:

2.8.1   Remarks

Before we procede with the proof of this result, we make a few remarks about it. Lighthill [18] notes that direct integrations for particular $\mathbf{f}(s)$ suggest that the actual error is $O(\epsilon)$. it is not known if the $\epsilon^{1/2}$ estimate is sharp. Nevertheless, the main point of the result is that the error is very small compared to any inverse power of $-\log\epsilon$. Note that if $L = \infty$, the error E becomes indeterminant, while if $l = \infty$ the error remains$O(\epsilon^{1/2})$ but the integral on the right of (2.113) diverges logarithmically. For un-dudlating zero-thrust flagella of finite length we can expect the theorem to give a good approimatiion provided that the length exceeds several wavelengths. On the other hand, if the flagellum pushes a large cell body and is therefore delivering non-zero thrust, the resistance as the flagellum drifts backward relative to its zero-thrust motion is computed by considering Stokes flow with this drift velocity past the wavy surface. For this calculation the series expansions of [3] and [4] must be used, proceeding in powers of $\Delta = [-\log(\epsilon/2]^{-1}$. Thus the error of actually computing resistance coefficients is not indicated by (2.113).

Even in the case of zero-thrust swimming, (2.113) indicates that there is no exactly *local* relation between velocity and resistance. The velocity of the fluid at a given section depends upon all point so the flagellum. A semi-local "range of influence" for the force ata given section is roughly several wavelengths of motion. This range of influence increases with l until the entire flagellum is affected. From these deductions Lighthill concludes that the rational approach to flagellar hydrodynamics must account for the quite different Stokes flows created in the zero thrust and non-zero thrust cases. The latter are strongly non-local, the former at most "semi-local"on the scale of the wavelength.

It is worth noting how the form of (2.113) reflectsthe approximate local theory of resistance coefficients. If in our expressions (2.74) and (2.81) defining K_T, K_N, we replace $L_1 L_2$ by $\delta_2 = a^2 e/4$, then K_T^{-1} vanishes and we are left with only a normal resistance with $K_N = 4\pi\mu$. This shows that the analysis leading to (2.113) isolates just enough of the flagellum to extract the slight dominance of K_N as a local effect. The rest of the contribution for the forces, both normal and tangential, is put into the non-local integral.

As a final point it is worth noting that, since we might expect that in applications the *velocity* rather than the force to be prescribed, the analysis thus poses an interesting integral equation for $\mathbf{f}$.

$f(\epsilon) = O(g(\epsilon))$ as $\epsilon \to 0$ if there are constants A, ϵ_0 such that $|f| < A|g|$ for $0 < \epsilon < \epsilon_0$.

2.8.2   Proof of the theorem.

For now the reader is referred to Chapter 6 of *mechanics of Swimming and Flying* to see the main steps. Note that the notation there is slightly different. Eventually a simplified version of the proof, which corrects some typos, will appear in this subsection.

2.8.3   Application to helical waves

The application of the theorem to an infinite zero-thrust helical flagellum is significant because of its biological relevance as well as because of the remarkable fact that the integral equation for $\mathbf{f}$ posed by (2.113) can be solved by inspection. Indeed, for a helical flagellum (2.97) the force distribution should be invariant under the symmetry of the helix, in particular under $s \to s + \Delta s, x \to x + \alpha \Delta s, y \to y \cos \theta - z \sin \theta, z \to z \cos \theta + y \sin \theta$, where $\theta = k\Delta s$. This suggests that for zero mean thrust to prevail, $\mathbf{f}$ will have y and z components that are linear combinations of $\sin ks$ and $\cos ks$, whereas the x component, necessarily constant, must vanish. The appropriate phase can be cetermined by inspection and Lighthill [18] finds that the ncessary boundary velocity is generated by taking

$$\mathbf{f}(s) = (0, h \sin ks, -h \cos ks), \tag{2.114}$$

were h is a constant. The velocity of the points of flagellum through the fluid is $\mathbf{w} = (U + V)\mathbf{i} - Q\mathbf{t}$, so the velocity of the fluid at the body is $(-U, Qbk \sin ks, -Qbk \cos ks)$. Now, with $\mathbf{t} = (\alpha, -bk \sin ks, bk \cos ks)$

$$\mathbf{f}_n = \mathbf{f} - \mathbf{f} \cdot \mathbf{tt} = h\alpha(bk, \alpha \sin ks, -\alpha \cos ks). \tag{2.115}$$

It is then possible to bring(2.113) into the following form:

$$(-U, Qbk \sin ks, -Qbk \cos ks) = \frac{h\alpha}{4\pi\mu}(bk, \alpha \sin ks, -\alpha \cos ks)$$

$$+ \frac{1}{8\pi\mu} \int_{G<\delta} G^{-3}[(0, h \sin ks, -h \cos ks)G^2 - bh\mathbf{G} \sin k(s - s_0)\rho]ds \tag{2.116}$$

where

$$\mathbf{G} = [\alpha(s - s_0), b(\cos ks - \cos ks_0), b(\sin ks - \sin ks_0)]. \tag{2.117}$$

The x-component of (2.116) thus gives, with $k(s - s_0) = \theta$ in the integrand, the zero thrust swimming velocity in the form

$$U_0 = \frac{h\alpha bk}{4\pi\mu}\Big[\int_{k\delta}^{\infty} \frac{\theta \sin \theta}{H^3(\theta)}d\theta - 1\Big], \tag{2.118}$$

where $H(\theta) = [\alpha^2\theta^2 + 2(1 - \alpha^2)(1 - \cos\theta)]^{1/2}$. Similarly the other two components yield

$$Qbk = \frac{h\alpha^2}{4\pi\mu} + \frac{h}{4\pi\mu}\int_{k\delta}^{\infty}\frac{\cos\theta}{H(\theta)}d\theta + \frac{h(1 - \alpha^2)}{4\pi\mu}\int_{k\delta}^{\infty}\frac{\sin^2\theta}{H^3(\theta)}d\theta. \qquad (2.119)$$

Thus, given the force, we determine the swimming speed and the helical wave speed.

Calibration of resistance coefficients

We now see what information we can get from this helical, zero-thrust solution if we try to express the equilibrium using force coefficients. Recall that our aproximate local theory gave

$$K_T = \frac{4\pi\mu}{\log(4L_1L_2/a^2) - 1}, \; K_N = \frac{8\pi\mu}{\log(4L_1L_2/a^2) + 1} \qquad (2.120)$$

Thus the combination $\kappa \equiv 4\pi\mu/K_N - 2\pi\mu/K_T = 1$

For the helical flagellum, the tangential component of velocity is

$$u_t = (-U, Qbk\sin ks, -Qbk\cos ks)\cdot(\alpha, -bk\sin ks, bk\cos ks) = -\alpha U_0 - Qb^2k^2, \qquad (2.121)$$

whereas the tangential force is $-bkh$, and so by definition

$$K_T = bkh[\alpha U_0 + Q(1 - \alpha^2)]^{-1}. \qquad (2.122)$$

Similarly

$$K_N = h\alpha bk(Q\alpha - U_0)^{-1}. \qquad (2.123)$$

What then is $\kappa = 4\pi\mu/K_N - 2\pi\mu/K_T$ in the helical case? We get

$$\kappa = 2\pi\mu\Big[\frac{Qb^2k^2\alpha + (\alpha^2 - 2)U_0}{h\alpha bk}\Big]. \qquad (2.124)$$

We thus have

$$\kappa = \frac{\alpha^2 - 2}{2}\Big[\int_{k\delta}^{\infty}\frac{\theta\sin\theta}{H^3(\theta)}d\theta - 1\Big] + \frac{\alpha^2}{2} + \frac{1}{2}\int_{k\delta}^{\infty}\frac{\cos\theta}{H(\theta)}d\theta$$

$$+ \frac{(1 - \alpha^2)}{2}\int_{k\delta}^{\infty}\frac{\sin^2\theta}{H^3(\theta)}d\theta. \qquad (2.125)$$

This may be brought into the form

$$\kappa \approx \kappa(\alpha) = \frac{\alpha^2}{2}I_1(\alpha) + \frac{1}{2}I_2(\alpha) + (2 - \alpha^2)/2, \qquad (2.126)$$

where $I_{1,2}$ are both integrals which exist as $k\delta \to 0$, so that for small $k\delta$ we have

$$I_1 \approx \int_0^{\infty}\frac{\theta\sin\theta - \sin^2\theta}{H^3}d\theta + 1, \qquad (2.127)$$

$$I_2 = \int_0^\infty \frac{\sin^2\theta + \cos\theta(\alpha^2\theta^2 + 2(1-\alpha^2)(1-\cos\theta) - 2\theta\sin\theta}{H^3} d\theta. \quad (2.128)$$

From these results it is easy to see that $\kappa(1) = .5$. We show the variation for other α in Figure 2.3.
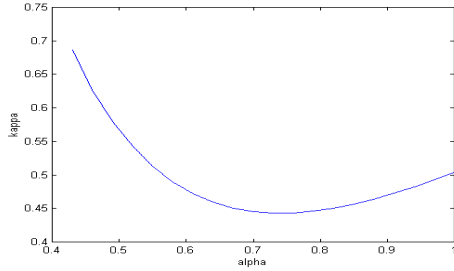

Figure 2.3: $\kappa = 4\pi\mu/K_N - 2\pi\mu/K_T$ as a function of α for the helical flagellum.

Note that the Gray-Hancock value of 1 not a good representative constant value. Shack et al. [?] have proposed, on the basis of the theory of Cox [4],

$$K_T = \frac{2\pi\mu}{\log(2q/a)}, K_N = \frac{4\pi\mu}{\log(2q/a) + \frac{1}{2}}, \quad (2.129)$$

where $q = \frac{1}{2\pi e^\gamma}\lambda \approx .09\lambda$ for force distributions with wavelength $2\pi/\lambda$, γ being Euler's constant $0.577\ldots$.. For these coefficients $\kappa = 1/2$, which from Figure 2.3 is not an unressonable value. But in any case the impossibility of a universal constant value of κ can not be achieved, and this calibration is an indication of the impossibility of an exact, fully local resistive force theory.

2.9   Ciliary propulsion

A second basic swimming mechanism in the Stokesian realm involves the collective use of many small hairlike organelles called *cilia*. Although flagella and cilia of the eukaryotic organisms (e.g. protozoans, algae, and the multicelluar organisms) are apparently identical in ultrastructure, we have used the term *flagellum* when there is only one, or a small number of these appendages on a cell, and in spermatozoans and the flagellates, and will use *cilia* to denote large numbers of them on the cell, as in the opalinates and the ciliates (see the discussion of the biology of locomotion in chapter ??). The ciliated organisms tend to have bodies which are larger that the

cell bodies of the spermatozoans by an order of magnitude. Cilia tend to be shorter that flagella, however, which puts their hydrodynamics firmly in the Stokesian realm.

Bacteria have organelles which are also called flagella, but they are very different in ultrastructure and physiology, see ??. Also, the term *cilia* is used in connection with various ciliated tissues in metazoans (many-celled animals), and are found in the lining of our respiratory tract. But in these cases there is usually only one or a small number of cilia per cell.

Because of the proximity of a cilium to the cell wall, we can expect to find considerable interaction between the two. Thus we might expect to see differences between the movements of cilia and flagella proper. This, and the larger size of the cell, suggest that ciliary locomotion might have some adaptive advantages for larger cell bodies. Both flagellary and ciliary modes are widespread, so both are evidently successful strategies, and one can speculate on what trade-offs the distinctly different morphology might represent.

In one sense the proliferation of hairlike appendages is natural to the Stokesian realm, purely on the basis of the efficient use of material. The movement of a cylindrical rod of radius A and length L will, according to our approximate local theory, generate a force of order $\mu U L / \log(L/A)$. If the cylinder is broken up into $N \gg 1$ thin hairs of length L and radius $a = A/\sqrt{N}$, the total force on all the hair is of order $N\mu U L / \log(L\sqrt{N/A})$. This shows that a Stokesian parachute could be made efficiently of hairs. Such a strategy if probably seen in seed dispersal by plants such as dandelions, and by the membraneless hairs utilized as wings by certain minute flying insects.

Such considerations alone may not, however, suffice to explain the possible value of ciliary propulsion to the organism. We have seen from the Gray-Hancock theory that the mechanical efficiency of a flagellum depends on resistances through their *ratio* ρ, and the efficiencies of single flagella tend to be in the range $1 - 10\%$, with 4% typical. Given the prevalence of both strategies, it is perhaps not surprising that efficiencies in ciliary locomotion are comparable, see [20] and Exercise 2.6. Although these estimates are approximate, the efficiencies might be regarded as unexpectedly high in view of the adverse effects of interaction with the cell wall.

Perhaps the most compelling advantage of the ciliary strategy is its flexibility. A large number of essentially identical organelles can be distributed and coordinated as a sort of standard "ciliary carpet". Pieces of this carpet can be arranged as needed on a cell to optimally move a cell of given size and shape. A possible disadvantage of the ciliary mode is the clear need to coordinate the motion of a large number of organelles.

2.9.1   The motion of an individual cilium

Typical parameters of a cilium are: length $\sim 10^{-3}$ cm $= 10$ μm (1 μm $= 10^{-4}$ cm); diameter $\sim .25$ μm; tip speed $\sim 0{,}2$ cm/sec; beat frequency $\sim$ 30 cycles/sec. A typical beat cycle consists of two parts, an *effective stroke* and a *recovery stroke*, see Figure 2.4.

See figure page 64 of MS&F.

Figure 2.4: The stroke sequence of a cilium. (a) Effective stroke. (b) Recovery stroke.

The effective stroke may take somewhat less than 1/2 a cycle. A Reynolds number for a single cilium based on length and tip speed is about 0.02. The Reynolds number based upon ciliary diameter is smaller by a factor of 1/40.

Cilia may beat in a vertical plane, as we imply in Figure 2.4, but in some cases the recovery stroke involves out-of-plane sideways movements. Cilia may move as a bundle, comprising a *compound cilium*. Helical waves are also observed.

In any case the basic motion seems sound from a fluid dynamic viewpoint. The effective stroke tends to be broadside on, developing the larger force associated with the resistance coefficient K_N. During the recovery the motion tends to be tangential, and therefore to involve the somewhat smaller resistance coefficient K_T.But it should be borne in mind that there are many variations of the basic stroke and the foregoing remarks have not addressed the interaction of the cilium with the wall.

2.9.2   Metachronal coordination

An important aspect of ciliary locomotion is the manner in which the cycles of cilia are coordinated as a function of position. Observations of the surface of a ciliate show *metachronal waves* of coordination in the beating pattern. These waves, which flow across the cell body with well-defined wave speed and wave length, have several forms. Figure 2.5a shows *symplectic metachrony*, in which the cilia tips in the effective stroke move in

the same direction as the metachronal wave. *Antiplectic metachrony* occurs when these move in opposite directions, see Figure 2.5b. It is observed that symplectic metachrony involves less horizontal movement of the cilia tips than does antiplectic metachrony. The phase of the cilia may also vary in the lateral direction, so that waves may propagate obliquely or even at right angles to the plane of the beat. The terminology used is summarized in Figure 2.6.

See figure page 65 of MS&F.

Figure 2.5. Metachronal coordination. (a) Symplectic, side view, planar motion. (b) Antiplectic.

See figure page 65 of MS&F.

Figure 2.6: The terminology for an array of cilia, top view. (After Blake and Sleigh [21]).

A typical protozoan with symplectic metachrony is the species *Opalina ranarum*, a disc-shaped organism inhabiting the gut of a frog. It is about 200 μm thick and the cilia are 10 μm in length, arranged in rows 3 μm apart. Within each row the distance between cilia is about 0.3 μm. Beat frequency is about 5 cycles per second. The metachronal wavelength is 30 to 50 μm and the metachronal wave speed (the speed of the crests) is 100-200 μm/sec. The cell swimming speed is about 50 μm/sec, or about 1/4 of the wave speed.

Typical dexioplectic metachrony is seen in *Paramecium* (which, together with *Opalina*, has been widely studied in connection with ciliary locomotion). This cigar-shaped protozoan, roughly 200 μm long, has cilia of length 12 μm arranged in a square array about 2-3 μm apart, beating with a frequency of 20-30 cycles/sec. The metachronal wavelength is only 10 μm, the wave speed being about 200 μm/sec. Whereas the last figure is comparable to *Opalina*, the swimming speed of *Paramecium* is 1000-2000 μm/sec, 5 to 10 times the wave speed. Models for ciliary propulsion must account for this wide range of behavior among ciliates.

2.9.3   The envelope model

A natural way to model the effect of cilia on the fluid, and one that is particularly appropriate to this discussion, is to replace the surface of waving cilia tips by a continuous sheet, thus realizing the stretching, waving swimming sheet first studied by G.I. Taylor. This *envelope* model takes the view that a closely spaced array of beating cilia will move the nearby fluid very much as if the cilia tips were a surface. Note that this is essentially a consequence of Stokes' paradox, indicative of the enormous hydrodynamics range of a long slender object has in a Stokesian fluid.

In the envelope model the motion of the individual cilia, apart from the locus of tips, plays no role. The tip loci are assumed to provide adequate parameters for the metachronal waves. It is important to note that these parameters need not be constant over the cell body (as they were assumed to be for the sheet itself). We shall however, in the present section, keep the assumption of constant parameters and simply reinterpret the results we have for the swimming sheet in the context of the envelope model.

The model assumes that the sheet is impermeable to the fluid, although of course this is not exactly true, particularly in the case of antiplectic metachrony, where the tips are widely spaced during the effective stroke (Figure 2.4b).

We shall use the result given earlier for the swimming sheet. The coordinates of the sheet satisfy

$$x_s = x + a \cos \xi, \ y_s = b \sin \xi, \ \xi - kx - \omega. \tag{2.130}$$

Taking a typical point by setting $x = 0$ we have

$$(bx_s - ay_s \sin \phi)^2 + a^2 y_s^2 \cos^2 \phi = a^2 b^2 \cos^2 \phi. \tag{2.131}$$

The orbit is thus a ellipse. With $x_s = aX, y_s = bY$ we get

$$X^2 - 2XY \sin \phi + Y^2 = \cos^2 \phi. \tag{2.132}$$

The form of the locus for various $\phi, b/a$ can thus be found, and we give some examples in Figure 2.7.

See figure page 67 of MS&F.

Figure 2.7: Tip loci in the envelope model, $\omega, a, b > 0$.

Let us now relate the parameters of the sheet to the metachronal wave. The uniform flow induced by the sheet and the rate of working of the sheet are given by

$$U = \frac{1}{2}\omega k(b^2 + 2ab\cos\phi - a^2), \; W = \mu\omega^2 k(a^2 + b^2). \qquad (2.133)$$

Recall that $U > 0$ means that the sheet swims to the left. This occurs here if $\phi = 0$ and $b > (\sqrt{2} - 1)a$. That is, the sheet swims in a direction opposite to the metachronal wave if cilia tips move mainly up and down. This is in rough agreement with observations of *Opalina*. If $\phi = \pi$ and $a > (\sqrt{2}-1)b$, so the main tip motion is horizontal, the sheet moves to the right, in the direction of the metachronal waves, in accord with observations of *Paramecium*.

Given U and W, we can seek to maximize $|U|$ for a given W. We suppose that ω and k are fixed, and set $(a,b) = R(\sin\theta, \cos\theta)$, with R also fixed. We then seek extremals of $\cos^2\theta + 2\cos\theta\sin\theta\cos\phi - \sin^2\theta = \cos 2\theta + \cos\phi\sin 2\theta$, with respect to variations of θ, ϕ. Differentiating with respect to ϕ we get $-\sin\phi\sin 2\theta = 0$, so either $\phi = 0$ or π, of else $\sin 2\theta = 0$. The derivative with respect to θ gives $-2\sin 2\theta + 2\cos\phi\cos 2\theta = 0$, so that either $\sin 2\theta = 0$ *and* $\cos\phi = 0$, or else one of the following two cases holds: $\phi = 0, \tan 2\theta = 1$ or $\phi = \pi, \tan 2\theta = -1$. The first choice implies that either $\sin\theta$ of $\cos\theta$ vanishes, so that either a or b is zero. The second choice ($\phi = 0$) implies $2\tan\theta = 1 - \tan^2\theta$, so either $a = (\sqrt{2} - 1)b$ or else $b = (1 - \sqrt{2})a$. The last choice ($\phi = \pi$) implies $2\tan\theta = \tan^2\theta - 1$, so either $a = (1 - \sqrt{2})b$ or else $b = (\sqrt{2}-1)a$. As we may assume that $a, b > 0$ without loss of generality, we obtain swimming speeds $\pm\frac{1}{2}\omega kR^2$ if a or b vanishes, and

$$U = \frac{1}{\sqrt{2}}\omega kR^2, \; \phi = 0, a = (\sqrt{2} - 1)b, \text{ (symplectic)}, \qquad (2.134)$$

$$U = -\frac{1}{\sqrt{2}}\omega kR^2, \; \phi = \pi, b = (\sqrt{2} - 1)a, \text{ (antiplectic)}. \qquad (2.135)$$

Thus, a speed gain of about 41% results from a combination of vertical and horizontal movements of the envelope, and the optimal parameters fall in a range already noted to be consistent with observation.

2.9.4 Macrostructure

We consider now the nature of the flow field about a ciliated organism consisting of a cell body covered with some arrangement of cilia. Define L a s a typical cell diameter ~ 200 μm, $\lambda = $ the metachronal wavelength ~ 40 μm, $l = $ cilium length ~ 10 μm. These lengths form a decreasing sequence and therefore suggest an envelope theory relying on the ordering $L \gg \lambda \gg l$. Recall that the hydrodynamic effects of the sheet extend outward a distance $O(\lambda)$ from the envelope surface.

With this ordering, it becomes possible to consider the *modulation* of the parameters of the sheet on the scale L of the cell body. We may then say that the sheet parameters are slowly-varying relative to the scale λ of the metachronal waves. This give the cell body a *macrostructure*, defined by the functions modulating the parameters and determining their values over the surface of the cell, see Figure 2.8.

See figure page 69 of MS&F.

Figure 2.8: Macrostructure of a ciliate, $L \gg \lambda \gg l$.

While the sheet surface then essentially replaces the cell surface, it must be understood that a thin *sublayer*, or thickness l, is actually present and the motions of the cilia within it must determine the envelope parameters. One can of course imagine another approach involving calculations within the sublayer (see the following subsection), for which the flow field set up by the cilia emerges as the outer edge of the sublayer. Here, we disregard the sublayer itself but regard the conditions out a distance $O(\lambda)$ from the envelope surface as hydrodynamically equivalent to that produced by the sublayer. This viewpoint was the basis for comprehensive theory of ciliary propulsion developed by Brennen [25], [24].

From the elements of the sheet theory we can piece together the flow field on the scale of the cell body. We now refer to the "surface of the cell" where

we actually mean the outer edge of the decaying flow structures induced by the oscillating envelope.

First note that the velocity of the fluid on the surface of the body involves the cell swimming velocity , its angular velocity, and the velocity produced by the sheet itself (equal to minus the local velocity of swimming of a piece of the sheet). In principle, we must also include the modulation of the mass flux $f_m = -\frac{1}{2}\omega\beta b$. The partial derivative of this quantity, in the tangent plane at the surface of the cell in a direction orthogonal to the crests of the waves, must be minus the normal component of velocity supplied by the modulated envelope at its outer edge. Since the modulation is on the scale L, whereas $k = 2\pi/\lambda$, the normal flow so induced will be $O(\lambda/L)\mathbf{U}$ and so is negligible in our ordering of the lengths λ, L.

Therefore, relative to the moving cell, the velocity of the fluid at the cell boundary is

$$\mathbf{u} = \mathbf{u}_c = k^{-1}U\mathbf{k} + \mathbf{r} \times \Omega. \tag{2.136}$$

This would be replaced by the no-slip condition $\mathbf{u}_c = 0$ if we were dealing with a rigid, non-rotating body. Relative to am observer stationary with respect to the distant fluid, the velocity of a point on the cell body is just $\mathbf{U}_{sc} + \mathbf{u}_c$ where $\mathbf{U}_{sc}$ is the swimming velocity of the cell.

While this last boundary condition would appear to have captured the effects of the envelope, it is in fact incomplete owing to the momentum flux components we computed for the sheet, whose modulation will give rise to effective surface stresses, in the same way that the waving cilia present an effective surface velocity. The fact that these *envelope stresses* turn out to be as important to the macrostructure of the flow as the tangential flow induced by the sheet, is an important fact emerging from Brennen's analysis.

The tangential and normal momentum fluxes can be written as $\alpha_t\mathbf{k}, \alpha_n\mathbf{k}$, where $\mathbf{k}$ is the wave number vector for the metachronal waves, lying in the tangent plane to the cell surface, and $\alpha_t = -2\mu\omega\gamma b$, $\alpha_n = \mu\omega\beta b$. Consider now a small, simply-connected domain D on the cell surface, bounded by a curve C which is positively oriented relative to the outer normal $\mathbf{n}$ of the cell surface. The size of D should be such that it is large enough to encompass many metachronal waves, but is still small compared to the body size L. At each point of C, let $\mathbf{t}_1$ be a tangent vector which is also an outer normal to C, and let $\mathbf{t}_2$ be another tangent vector, orthogonal to $\mathbf{t}_1$ and pointing in the direction of the tangent vector of the curve C, so that $\mathbf{n} = \mathbf{t}_1 \times \mathbf{t}_2$ on C.

We then define the effective envelope stress as

$$\sigma_{env} = k^{-1}\mathbf{k}\sigma_t + \mathbf{n}\sigma_n, \tag{2.137}$$

where

$$\int_D (\sigma_t, \sigma_n)dS = \oint_C (\alpha_t, \alpha_n)\mathbf{k} \cdot \mathbf{t}_1 ds. \tag{2.138}$$

Using the definition of $\mathbf{t}_{1,2}$ and Stokes' theorem, we then have

$$\oint_C \alpha_{t,n} \cdot \mathbf{t}_1 ds = \oint_C \alpha_{t,n}(\mathbf{n} \times \mathbf{k}) \cdot \mathbf{t}_2 ds = \int_D \mathbf{n} \cdot [\nabla \times (\alpha_{t,n} \times \mathbf{k})] dS. \quad (2.139)$$

Thus

$$\sigma_{t,n} = \mathbf{n} \cdot [\nabla \times (\alpha_{t,n} \times \mathbf{k})]. \quad (2.140)$$

2.9.5   The ciliated sphere

We now carry out the construction of the flow field about a ciliated sphere, as shown in Figure 2.9.

See figure page 70 of MS&F.

Figure 2.9: The ciliated sphere.

We suppose that ω, k and ϕ are constant, that the crests of the metachronal waves are the circles of constant θ, as in the figure, and that $a = a_0\sqrt{\sin\theta}, b = b_0\sqrt{\sin\theta}$. The net force exerted *on the sphere* in the x direction is then

$$F = 2\pi r_0^2 \int_0^\pi (\sin^2\theta\sigma_t - \sin\theta\cos\theta\sigma_n)d\theta, \quad (2.141)$$

where r_0 is the radius of the sphere. In the spherical coordinate system we find, from (2.140) that

$$\sigma_t = -2\mu\omega ka_0b_0\sin\phi\Big(\frac{1}{r_0\sin\theta}\frac{\partial}{\partial\theta}\sin^2\theta\Big) = -4\mu\omega ka_0b_0r_0^{-1}\sin\phi\cos\theta. \quad (2.142)$$

$$\sigma_n = 2\mu\omega ka_0b_0r_0^{-1}cos\phi\cos\theta. \quad (2.143)$$

Consequently

$$F = -\frac{8}{3}\pi\mu\omega kr_0a_0b_0\cos\phi. \quad (2.144)$$

Thus, in steady swimming of the sphere, the Stokes flow will contain a Stokeslet representing the corresponding force $-F$ *applied to the fluid*. The fluid velocity seen by the stationary observer then has the form of a sum of

this Stokeslet and the remaining component of Stokes flow past a sphere, namely an axial dipole:

$$\mathbf{u} = \frac{F}{8\pi\mu}\left(\frac{\mathbf{i}}{r} - \frac{\mathbf{r}\cos\theta}{r^2}\right) + Ar_0^3\left(\frac{\cos\theta}{r^2}\right), \tag{2.145}$$

Here A is to be adjusted to satisfy the boundary conditions on the cell surface.

The latter are, if $\mathbf{U}_{sc} = U_{sc}\mathbf{i}$,

$$u_\theta = (U_{sc} + U_0)\sin\theta, \ u_r = -U_{sc}\cos\theta, \tag{2.146}$$

where $U_0 = \frac{1}{2}\omega k(b_0^2 + 2a_0b_0\cos\phi - a_0^2)$. (Note that our choice of variation of a, b was chosen to simplify both the boundary condition on u_θ and the calculation of F .)

From (2.145) and (**??**) we have

$$\frac{F}{8\pi\mu} - A = U_{sc} + U_0, \ \frac{F}{4\pi\mu} + 2A = U_{sc}. \tag{2.147}$$

Thus

$$U_{sc} = -\frac{2}{3}U_0 + \frac{F}{6\pi\mu r_0} = -\frac{1}{3}\omega k(b_0^2 + \frac{10}{3}a_0b_0\cos\phi - a_0^2). \tag{2.148}$$

Note that if $a_0 = 0$, the sheet swims at two-thirds of the velocity of an infinite sheet with these parameters. We also find that $|U_{sc}|/[\omega k(a_0^2 + b_0^2)]$ has a maximum value of about 0.648 compared to 0.707 for the infinite sheet. A number of examples have been worked out by Brennen [25], who compares the predicted swimming speeds with observations.

We now compare the ratio of the maximum swimming speed to the phase speed, equal to $0.648k^2(a_0^2 + b_0^2)$, with observations. if we take $a_0^2 + b_0^2$ to equal one-fourth of the square of the cilium length, then for *Opalina* the ratio is $(2\pi)^2(0.65/4)(10^2/40^2) = .40$. The observations indicate that $k|U_{sc}|/\omega = 0.25$, so the theory is reasonably close. For *Paramecium* the estimates given by the envelope theory are off by an order of magnitude, and it is believed that the failure of the envelope model in that case is due to inaccurate calculation of the envelope parameters, probably associated with the tip separation in antiplectic metachronism. Intuitively, when tips separate during the effective stroke, the cilia should be more effective because of reduced cilium-cilium interaction, and this could account for the higher swimming speeds which are observed in *Paramecium*. Also tip separation should allow fluid to circulate into the sublayer, making the assumption of an impenetrable surface untenable. With these points in mind, we turn now to a brief discussion of the flow field at the level of the sublayer.

2.9.6 Microstructure: the sublayer

Unchanged from pages 72-74 of MS&F. To be added later.

2.10   Exercises

2.1. Show that, if $\mathbf{u}_i, i = 1, 2, 3$ denotes the velocity field given by (2.4) with $\mathbf{a} = \mathbf{i}_1, \mathbf{i}_2, \mathbf{i}_3$ respectively and the same function χ in each case, then $x_1\mathbf{u}_1 + x_2\mathbf{u}_2 + x_3\mathbf{u}_3 + 2\nabla\chi$ is divergence-free and has the form of the first term in (2.12) with $P = \chi$. Similarly, show that, if $\mathbf{u}_i, i = 1, 2, 3$ denotes the velocity field given by (2.8) with $\mathbf{b} = \mathbf{i}_1, \mathbf{i}_2, \mathbf{i}_3$ respectively and the same function ψ in each case, then $x_1\mathbf{u}_1 + x_2\mathbf{u}_2 + x_3\mathbf{u}_3$ is divergence-free and has the form of the second term in (2.12) with $T = \psi$.

2.2. Using the same basic approach as for the uniqueness proof for the Stokes equations, prove the following result: Let a finite rigid 3D body move with steady velocity $\mathbf{U}$ in a fluid otherwise at rest, From the steady Navier-Stokes equations for a fluid of constant density, prove that, if D denotes the drag on the body,

$$UD = \frac{\mu}{2}\int_V\left(\frac{\partial u_i}{\partial x_j} + \frac{\partial u_j}{\partial x_i}\right)^2 dV.$$

Here V is the domain exterior to the body. The quantity on the right is the total viscous dissipation in the fluid, so this is a mechanical energy equation, stating that the work done on the fluid by the body is equal to the rate of heating of the fluid by viscous dissipation. What conditions on the decay at infinity are needed in this proof? Show that, if the body surface is in motion with an arbitrary velocity $u_S(\mathbf{x})$, the viscous dissipation equals the rate of working of the surface S on the fluid.

2.3. (a) Show that a sphere of radius r_0 spinning with angular velocity Ω in Stokes flow experiences a viscous torque $-8\pi\mu r_0^3\Omega$. Using the form of solution given by (2.29) derive the Stokes drag law $D = 6\pi\mu r_0 U$, showing in the process that the pressure is responsible for $1/3$ of the total drag. In these problems you can use

$$\sigma_{r\theta} = \mu r\frac{\partial}{\partial r}\left(\frac{\partial u_\theta}{r}\right) + \frac{1}{r}\frac{\partial u_r}{\partial\theta},$$

$$\sigma_{rr} = -p + 2\mu\frac{\partial u_r}{\partial r},$$

together with the divergence conditions on $\mathbf{u}$.

2.4. Establish (2.39) and (2.41) using the definition of the stress tensor, the divergence theorem, and the properties of $\mathbf{u}_{1,2}$.

2.5. Let the motion of a helical flagellum be given by $(U + V)\mathbf{i} - Q\mathbf{t}$ plus a rotation $\left(0, -\Omega b\sin k(s + Qt), +\Omega b\cos k(s + Qt)\right)$. Show that the total thrust on length L of flagellum thrust T is given by

$$L^{-1}T = U[(K_T - K_N)\alpha^2 + K_N] + (V - \alpha\Omega k^{-1})[(K_T - K_N)(\alpha^2 - 1)].$$

Show also that the torque m_x about the axis (the x-component), defined by $\mathbf{i}\cdot\int_0^L[(0, b\cos k(s + Qt), -b\sin k(s + Qt))\times\mathbf{F}]ds$ is given by

$$\frac{m_x}{b^2 kL} = U\alpha(K_T - K_N) + (V - \alpha\Omega k^{-1})[\alpha(K_T - K_N) - \alpha^{-1}K_T].$$

From these two expressions, show that simultaneous torque and thrust balance, $T = m_x = 0$, is impossible for an isolated flagellum, in that when both expressions vanish we must have $U = V - \alpha\Omega k^{-1} = 0$. Thus swimming is posssible only if there is a passive body attached to the flagellum which can resist torque, or else there is surface rotation of the flagellum itself. Also a *keel*, i.e. an asymmetric weight distribution, can be used to obtain a restoring torque.

   2.6. Define an efficiency of the ciliated sphere by

$$\eta = \frac{6\pi\mu r_0 U^2}{W}.$$

Where W is computed by integrating $W_s = \mu\omega^2 k(a^2 + b^2)$ over the surface of the sphere. Show that, if $a^2 + b^2$ is distributed over the sphere in proportion to $\sin\theta$, $a^2 + b^2 = \sin\theta(a_0^2 + b_0^2)$, optimal efficiency is about

$$5\left(\frac{a_0^2 + b_0^2}{r_0\lambda}\right), \lambda = \frac{2\pi}{k}.$$

For a ciliate such as *Opalina*, we can take $r_0 = 80\ \mu$, $\lambda = 40\ \mu$m, and $a_0^2 + b_0^2 = 25\ \mu$m^2, in which case $\eta_{max} \approx 4$ percent. Extend (2.109) to the case of a flagellum attached to a head with resistance coefficient $K_N\delta$, making use of the swimming speed for that case (2.96).

References

[1] George Backus. A class of self-sustaining dissipative dynamos. *Annals of Physics*, 4, 1958.

[2] G.K. Batchlor. *An Introduction to Fluid Mechanics*. Cambridge University Press, 1967.

[3] G.K. Batchelor. Slender-body theory for particles of arbitrary cross0sectiion in Stokes flow. *J. Fluid mech*, 44, 419-440, 1970.

[4] R.G. Cox. The motion of long slender bodies in a viscous fluid. Prt I. General theory. *J, Fluid Mech.*, 44, 791-810, 1970.

[5] A.T. Chang and T.Y. Wu A note on the helical movement of micro-organisms. *Proc. Roy. Soc. Lond.*, A178, 327-346, 1971.

[6] Harley Flanders. *Differential Forms*. Academic Press, New York, 1963.

[7] John Happel and Howard Brenner. *Low Reynolds Number Hydrodynamics*. Prentice-Hall. Inc., Englewood Cliffs, N.J., 1965.

[8] Q.A. Ladyzhenskaya. *The Mathematical Theory of Viscous Incompressible Flow*. Gordon and Breach, New York, 1963.

[9] Sir Horace Lamb. *Hydrodynamics*. Cambridge University Press, sixth edition, 1932.

[10] L.D. Landau and E.M. Lifshitz. *Fluid Mechanics*, volume 6 of *Course in Theoretical Physics*. Pergammon Press, New York, second edition, 1987.

[11] L.M. Milne-Thomson. *Theoretical Hydrodynamics*. The Macmillan Company, New York, third edition, 1955.

[12] E.M. Purcell Life at low Reynolds number *Am. Jour. Phys.*, 45:3–11, 1977.

[13] P.H. Roberts. *An Introduction to Magnetohydrodynamics*. American Elsevier Publishing Company, Inc., New York, 1967.

[14] G.I. Taylor. Analysis of the swimming of microscopic organisms. *Proc. Roy. Soc. Lond.*, A209:447–461, 1951.

[15] G.I. Taylor The action of waving cylindrical tails in propelling microscopic organisms. *Proc. Roy. Soc. Lond.*, A211:225–239, 1952.

[16] E.O. Tuck. A note on the swimming problem. *Jour. Fluid Mech.*, 31:305–308, 1968.

[17] M.J.Lighthill *Mathematical Biofluiddynamics* S.I.A.M. vol 17. Regional Conference Series in Applied Mathematics. Society for Industrial and Applied Mathematics, Philadelphia,1975.

[18] M.J. Lighthill Flagellar hydrodynamics. *SIAM Rev.*, 18, 161-230, 1976.

[19] J. Gray *Animal Locomotion* W.W. Norton & Company, New York, 1968.

[20] A spherical envolope approach to ciliary propulsion. *J. Fluid Mech*, 46, 199–208, 1971.

[21] J.R. Blake and M.A. Sleigh Hydromeechanical aspects of ciliary propulsion. In *SFI*, 185–209, 1975.

[22] T. Y.-T. Wu, C.J. Brokaw, and C. Brennen *Swimming and Flying in Nature*, vols. I and II (denoted here by $SFI, SFII$). Plenum Press, New York, 1975.

[23] C. Brennen An oscillating boundary-layer theory for ciliary propulsion. *J. Fluid mech.*, 65, 799–824, 1974.

[24] C. Brennen Hydromechanics of propulsiion of ciliated microorganisms.

[25] C. Brennen In *SFI*, 235–251, 1975.